Title

Thermodynamic Studies to Support Extraction of Uranium from Seawater:

Author

Rao, Linfeng

Publication Date

2015-09-04

Thermodynamic Studies to Support Extraction of Uranium from Seawater

Fuel Cycle Research & Development

Prepared for
U.S. Department of Energy
Materials Recovery and Waste Form Development
Linfeng Rao
Lawrence Berkeley National Laboratory
September, 2015

FCRD-MRWFD-2015-000361

Revision 2
12/20/2012

APPENDIX E

FCT DOCUMENT COVER SHEET [1]

Name/Title of Deliverable/Milestone/Revision No.	Thermodynamic Studies to Support Efficient Extraction of Uranium from Seawater
Work Package Title and Number	Fuel Resources – LBNL FT-15LB031003
Work Package WBS Number	1.02.03.10
Responsible Work Package Manager	Linfeng Rao (signature on file) (Name/Signature)

Date Submitted 9/4/2015

Quality Rigor Level for Deliverable/Milestone[2]	☒ QRL-3	☐ QRL-2	☐ QRL-1 ☐ Nuclear Data	☐ Lab/Participant QA Program (no additional FCT QA requirements)

This deliverable was prepared in accordance with Lawrence Berkeley National Laboratory
(Participant/National Laboratory Name)

QA program which meets the requirements of
☒ DOE Order 414.1 ☐ NQA-1-2000 ☐ Other

This Deliverable was subjected to:

☒ Technical Review ☐ Peer Review

Technical Review (TR)	**Peer Review (PR)**
Review Documentation Provided	**Review Documentation Provided**
☐ Signed TR Report or,	☐ Signed PR Report or,
☐ Signed TR Concurrence Sheet or,	☐ Signed PR Concurrence Sheet or,
☒ Signature of TR Reviewer(s) below	☐ Signature of PR Reviewer(s) below

Name and Signature of Reviewers

Zhicheng Zhang (signature on file)

NOTE 1: *Appendix E should be filled out and submitted with the deliverable. Or, if the PICS:NE system permits, completely enter all applicable information in the PICS:NE Deliverable Form. The requirement is to ensure that all applicable information is entered either in the PICS:NE system or by using the FCT Document Cover Sheet.*

NOTE 2: *In some cases there may be a milestone where an item is being fabricated, maintenance is being performed on a facility, or a document is being issued through a formal document control process where it specifically calls out a formal review of the document. In these cases, documentation (e.g., inspection report, maintenance request, work planning package documentation or the documented review of the issued document through the document control process) of the completion of the activity along with the Document Cover Sheet is sufficient to demonstrate achieving the milestone. If QRL 1, 2, or 3 is not assigned, then the Lab/Participant QA Program (no additional FCT QA requirements) box must be checked, and the work is understood to be performed, and any deliverable developed, in conformance with the respective National Laboratory/Participant, DOE- or NNSA-approved QA Program.*

This page is intentionally blank.

SUMMARY

This milestone report summarizes the data obtained in FY15 on the major task of quantifying the binding strength of amidoxime-related ligands. Thermodynamic studies of the interaction between U(VI) and amidoxime ligand HL^{III} were studied to quantify the binding ability of U(VI) with amidoxime-related ligands and help to select grafting/reaction conditions so that higher yield of preferred amidoxime-related ligands is obtained.

Besides the thermodynamic task, structural studies on vanadium complexation with amidoxime ligand were conducted to help understand the extremely strong sorption of vanadium on poly(amidoxime) sorbents. Data processing and summarization of the vanadium system are in progress and will be included in the next milestone report.

CONTENTS

FIGURES

TABLES

1. INTRODUCTION

To improve the extraction efficiency and reduce the extraction cost, fundamental understanding of the coordination chemistry of the extraction process is necessary. Therefore, thermodynamic and structural studies need to be conducted to determine the stability constants of the complexes of uranium with a series of amidoxime-type ligands and understand the coordination modes. In FY15, one major task was undertaken, to conduct thermodynamic studies of the interaction between U (VI) and Amidoxime ligand HL^{III}. Besides, structural studies of vanadium/glutaroimide-dioxime complex were performed. This report presents the data on the major task in FY15.

2. RESULTS

2.1 Interaction between U(VI) and AO ligand C

To help the development of more efficient amidoxime-based sorbents, three amidoxime-related small molecules that represent the three moieties shown in Scheme 1a have been prepared and studied. By selecting different experimental conditions, each of the three ligands, including glutarimidedioxime (H_2L^I), glutardiamidoxime (H_2L^{II}), and glutarimidoxioxime (HL^{III}), were obtained in high yields, as shown in Scheme 1b. Thermodynamic and structural studies have previously been conducted for the complexation of U(VI) and other metal ions with H_2L^I and H_2L^{II}. Results showed that glutarimidedioxime (H_2L^I) and glutardiamidoxime (H_2L^{II}) both form strong complexes with uranyl in aqueous solution. In particular, the tridentate H_2L^I ligand forms such strong complexes with U(VI) that it can effectively compete with carbonate for U(VI) under seawater conditions.

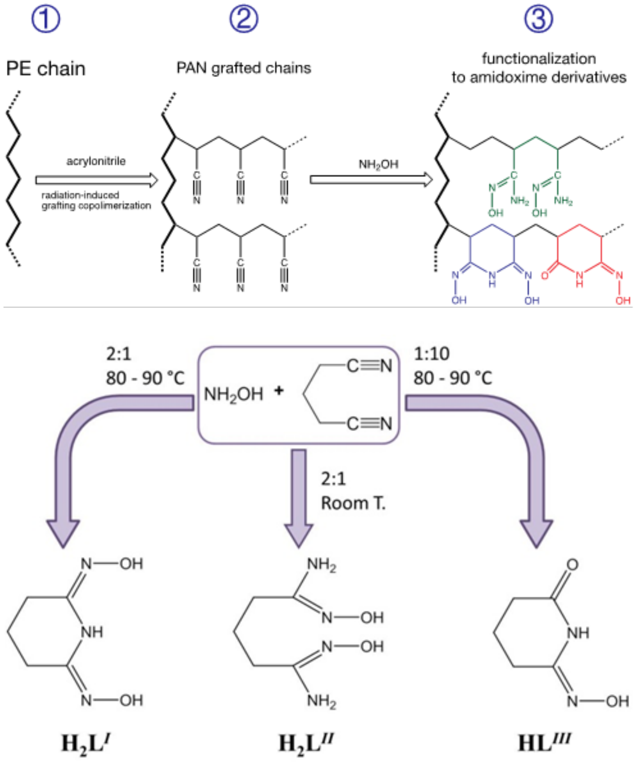

Scheme 1 (a, upper) Functionalization of polyacrylonitrile (PAN) sidechains with amidoxime derivatives; **(b, lower)** optimized experimental conditions for the synthesis of three amidoxime derivatives (glutarimidedioxime, H_2L^I; glutardiamidoxime, H_2L^{II}; glutarimidoxioxime, HL^{III}).

In FY15, thermodynamic measurements were conducted to quantify the binding ability of glutarimidoxioxime (HL^{III}), the third ligand in the series shown in Scheme 1b, towards U(VI). DFT calculations were performed to provide insight into the coordination mode in the U(VI)/HL^{III} complex. Results from this study on HL^{III}, in conjunction with the previous results on HL^{I} and HL^{III}, complete the systematic evaluation of the binding abilities of the possible configurations on the amidoxime-based sorbents, and help to optimize the process conditions to obtain the most efficient sorbent.

2.1.1 Stability constants

Figure 1 shows the potentiometric titrations for the complexation of U(VI) with HL^{III} using EDTA as a competing ligand. A number of speciation models were tried and the best fit of the experimental data was obtained with a model including the formation of a 1:1 complex $(UO_2L^{III})^+$ in the p[H] region of 3 – 5, with $\log\beta_{11} = (9.4 \pm 0.6)$ (Table 1). In the calculation, the equilibrium constants of UO_2^{2+} hydrolysis, EDTA protonation, and UO_2^{2+} complexation with EDTA, at $I = 0.5$ M (NaCl) were all included (see Table 1). These constants at $I = 0.5$ M (NaCl) were obtained from those at infinite dilution by using the *Specific ion Interaction Theory*. The constants at infinite dilution and $I = 0.5$ M (NaCl) are also listed in Table 1.

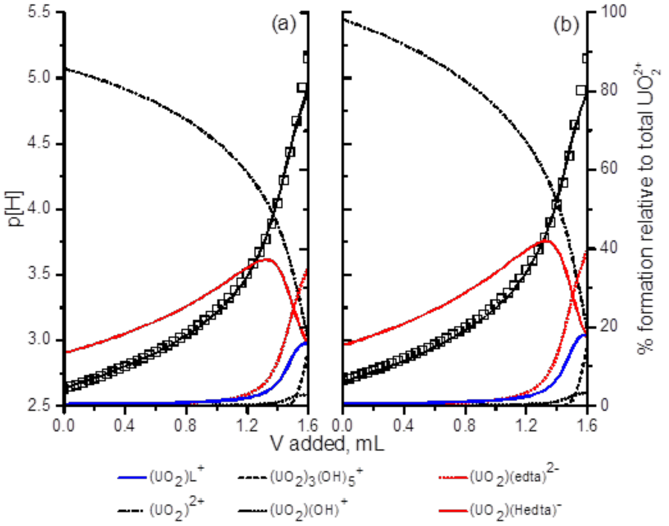

Figure 1. Potentiometric titrations for the complexation of U(VI) with HL^{III}. Left axis: p[H], □ experimental, - calculated. The full black curve is calculated by using the protonation constants in Table 1. Right axis: speciation of U(VI). Conditions: (a) $C_U^0 = 0.46$ mM, $C_H^0 = 4.82$ mM, $C_L^0 = 1.95$ mM, $C_{edta}^0 = 0.23$ mM, $C_{OH}^{titr.} = 20.0$ mM; (b) $C_U^0 = 0.41$ mM, $C_H^0 = 3.75$ mM, $C_L^0 = 1.21$ mM, $C_{edta}^0 = 0.21$ mM, $C_{OH}^{titr.} = 20.0$ mM.

Table 1. Thermodynamic data for the protonation and complexation of HL^{III} with U(VI) at infinite dilution ($\log \beta^0$) and I = 0.5 M ($\log \beta$). T = 298.15 K. Data for pertinent reactions from the literature are also listed. Bold numbers are data from this work.

Reaction	$\log\beta^0 \pm \sigma$	$\log\beta \pm \sigma$ (0.5 M NaCl)	$\Delta G \pm \sigma$ kJ/mol	$\Delta H \pm \sigma$ kJ/mol	$T\Delta S \pm \sigma$ kJ/mol
$H^+ + (L^{III})^- = HL^{III}$		**10.82 ± 0.01**	**− 61.77 ± 0.06**	**− 35.91 ± 0.02**	**25.86 ± 0.06**
$2H^+ + (L^{III})^- = (H_2L^{III})^+$		**12.0 ± 0.1**	**− 68.5 ± 0.6**	**− 42.03 ± 0.01**	**26.5 ± 0.6**
$H^+ + HL^{III} = (H_2L^{III})^+$		**1.2 ± 0.1**	**− 6.9 ± 0.6**	**− 6.12 ± 0.02**	**0.8 ± 0.6**
$UO_2^{2+} + (L^{III})^- = [(UO_2)L^{III}]^+$		**9.4 ± 0.6**			
$UO_2^{2+} + H_2O = [(UO_2)(OH)]^+ + H^+$	− 5.25 ± 0.24	− 5.65 ± 0.30			
$3UO_2^{2+} + 5H_2O = [(UO_2)_3(OH)_5]^+ + 5H^+$	− 15.55 ± 0.12	− 16.9 ± 0.2			
$UO_2^{2+} + edta^{4-} = [(UO_2)(edta)]^{2-}$	13.7 ± 0.2	11.3 ± 0.2			
$UO_2^{2+} + H^+ + edta^{4-} = [(UO_2)(Hedta)]^-$	19.61 ± 0.10	16.53 ± 0.12			
$H^+ + edta^{4-} = H(edta)^{3-}$	11.24 ± 0.03	10.12 ± 0.10			
$2H^+ + edta^{4-} = H_2(edta)^{2-}$	18.04 ± 0.04	16.07 ± 0.11			
$3H^+ + edta^{4-} = H_3(edta)^-$	21.19 ± 0.04	18.57 ± 0.11			
$4H^+ + edta^{4-} = H_4(edta)(aq)$	23.42 ± 0.06	20.35 ± 0.09			
$H^+ + OH^- = H_2O$		13.7004 ± 0.0003		− 56.5 ± 0.1	

2.1.2 Binding trends in ligand L^I, L^{II}, and L^{III}

The data from this work indicate that only one weak 1:1 complex between U(VI) and HL^{III} is formed, even at high ligand / uranium molar ratio (3:1 and 4:1 in Fig. 3). In contrast, a series of U(VI) complexes with different stoichiometries were observed for H_2L^I and H_2L^{II}. Besides, the complexation of HL^{III} with U(VI) is obviously much weaker than that of H_2L^I or H_2L^{II}. For the 1:1 complex with U(VI), the value of $\log\beta_{11}$ for $(UO_2L^{III})^+$ is (9.4 ± 0.6), about eight orders of magnitude lower than those for UO_2L^I (17.8 ± 1.1) and UO_2L^{II} (17.3 ± 0.3) (Table 2).

Table 1. Thermodynamic data for the protonation and complexation of three amidoxime-related ligands (I = 0.5 M NaCl, T = 298.15 K). Bold numbers are data from this work.

Ligand	Reaction	$\log\beta \pm \sigma$	$\Delta H \pm \sigma$ kJ/mol
Glutarimidoxioxime	**$H^+ + (L^{III})^- = HL^{III}$**	**10.82 ± 0.01**	**− 35.91 ± 0.02**
(HL^{III})	**$2H^+ + (L^{III})^- = (H_2L^{III})^+$**	**12.0 ± 0.1**	**− 42.03 ± 0.01**
	$H^+ + HL^{III} = (H_2L^{III})^+$	**1.2 ± 0.1**	**− 6.12 ± 0.02**
	$UO_2^{2+} + (L^{III})^- = [(UO_2)L^{III}]^+$	**9.4 ± 0.6**	
Glutardiamidoxime	$H^+ + (L^{II})^{2-} = (HL^{II})^-$	12.13 ± 0.12	− 52 ± 2
(H_2L^{II})	$2H^+ + (L^{II})^{2-} = H_2L^{II}$	24.19 ± 0.07	− 103 ± 3
	$3H^+ + (L^{II})^{2-} = (H_3L^{II})^+$	29.98 ± 0.07	− 124 ± 6
	$4H^+ + (L^{II})^{2-} = (H_4L^{II})^{2+}$	34.77 ± 0.07	− 151 ± 8
	$UO_2^{2+} + (L^{II})^{2-} = (UO_2)L^{II}$	17.3 ± 0.3	− 49 ± 6
Glutarimidedioxime	$H^+ + (L^I)^{2-} = (HL^I)^-$	12.06 ± 0.23	− 36.1 ± 0.5
(H_2L^I)	$2H^+ + (L^I)^{2-} = H_2L^I$	22.76 ± 0.31	− 69.7 ± 0.9
	$3H^+ + (L^I)^{2-} = (H_3L^I)^+$	24.88 ± 0.35	− 77 ± 6
	$H^+ + H_2L^I = (H_3L^I)^+$	2.12 ± 0.47	− 7 ± 6
	$UO_2^{2+} + (L^I)^{2-} = (UO_2)L^I$	17.8 ± 1.1	− 59 ± 8

2.1.3 Coordination Modes in U(VI)/L^{III} complex

The substantially weaker binding ability of HL^{III} than that of H_2L^I toward U(VI) is probably due to the lower denticity of HL^{III}. Previous studies have demonstrated that the cyclic H_2L^I (glutarimidedioxime, Scheme 1b) is a tridentate ligand and forms strong chelate complexes with UO_2^{2+} using the two oxime groups and the imino nitrogen. The chelate structure of the U(VI) complex with H_2L^I is particularly stabilized by a large conjugated ligand moiety that resulted from the relocation of the protons on the oxime groups and the deprotonation of the imino nitrogen. In contrast, the absence of a second oxime group in HL^{III} makes it less likely to form the same conjugated moiety and bind U(VI) in a strong tridentate mode. Therefore, HL^{III} probably binds U(VI) in a mono- or bi-dentate mode.

Attempts to obtain crystal structures of the $(UO_2L^{III})^+$ complex in this work were not successful. However, postulations on the coordination modes in this complex could be made, based on the information in the literature on the U(VI) complexes with related amidoxime ligands. Three possible coordination modes, including bi-dentate, mono-dentate, and η^2- coordination, could be suggested (Figure 2). The mono-dentate and η^2- coordination modes have been observed in U(VI) complexes with ligands structurally similar to HL^{III}. For example, the 1:1 U(VI) complex with acetamidoxime (AO), structurally similar to HL^{III}, is shown to have similar stability (log β_{11} = 10.6) to that of U(VI)/HL^{III} from this work (log β_{11} = (9.4 ± 0.6), Table 2). Also, X-ray crystallographic analysis in solid phase, combined with more recent DFT calculations, has shown that η^2-coordination exists in the U(VI)/AO complex, without the involvement of the $-NH_2$ group.

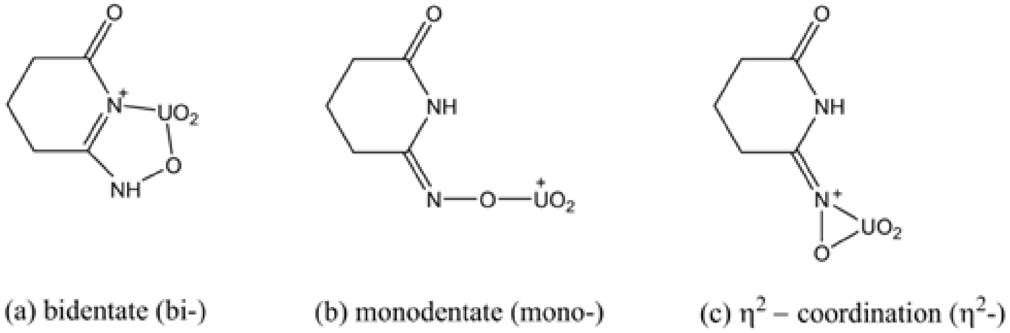

Figure 2. Possible coordination modes between HL^{III} and UO_2^{2+}.

In the absence of the crystallographic data on the structure of the $(UO_2L^{III})^+$ complex, DFT calculations were performed in this work to provide insight into the coordination mode(s) and help explain the binding strength and thermodynamic trends in the complexation of HL^{III} with U(VI).

The geometries of different hydrated complexes $[UO_2L^{III}(H_2O)_n\cdot m(H_2O)]^+$ (n = 0, 3, 4; m = 0, 1, 2; $n + m$ = 0 - 5) (structures *a* to *l* in Figure 3) were first optimized in the gas phase. An increased number of water molecules has been included to evaluate the effect of uranyl hydration on the preferential coordination mode with $(L^{III})^-$.

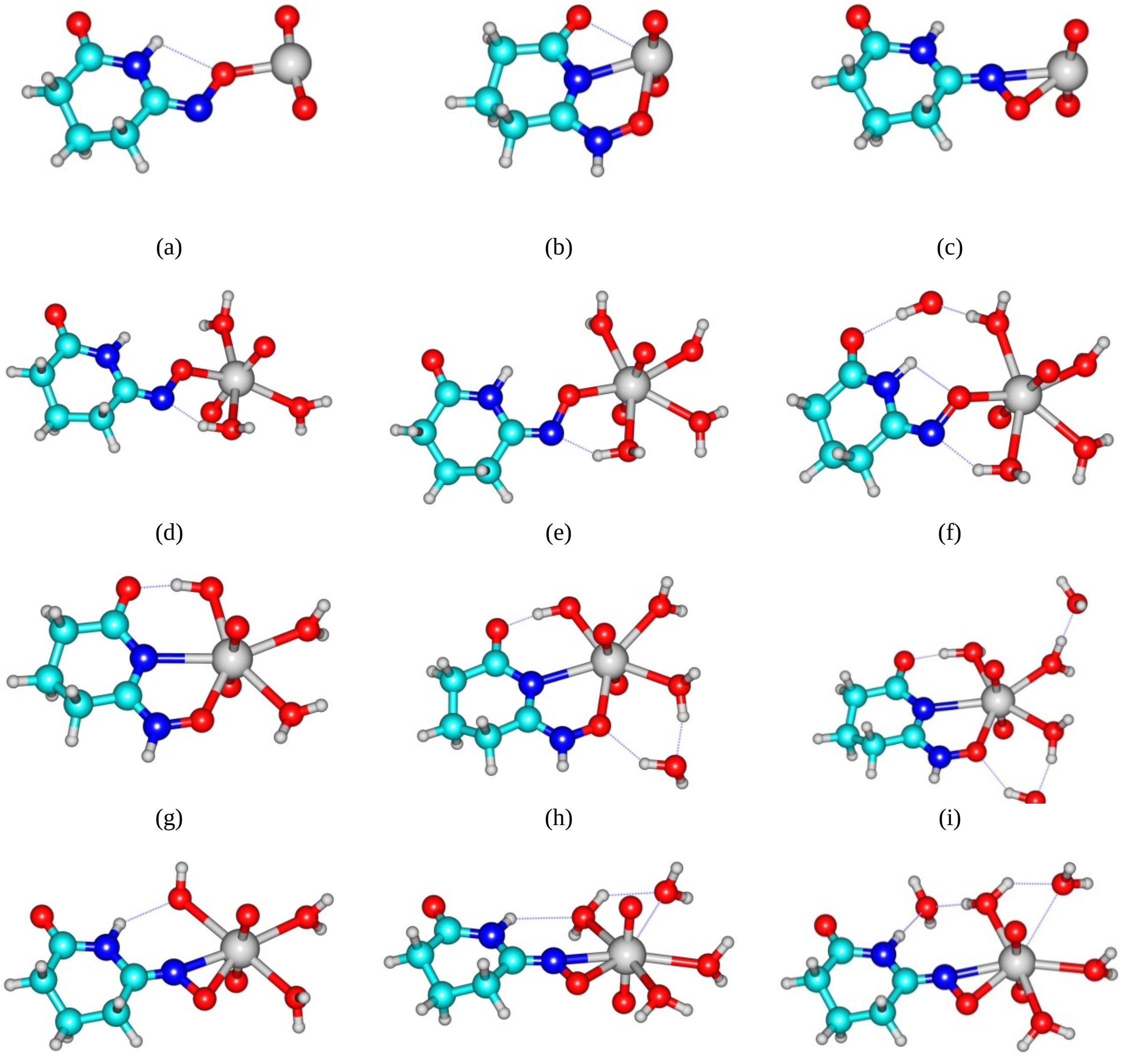
(a) (b) (c)
(d) (e) (f)
(g) (h) (i)
(j) (k) (l)

Figure 3. Optimized structures of the $[UO_2L^{III}(H_2O)_n{\cdot}m(H_2O)]^+$ complexes (n = 0, 3, 4; m =0, 1, 2; n + m = 0 - 5).

Then the structures were re-optimized in PCM water to take into account bulk solvation effects on the energy and structure of the reactants and products. In Table 3 are reported the ΔG values for reaction (1) for *a* - *c* and reaction (2) for *d* - *l*.

$$[UO_2]^{2+} + (L^{III})^- \rightarrow [UO_2L^{III}]^+ \qquad (1)$$

$$[UO_2(H_2O)_5]^{2+} + (L^{III})^- \rightarrow [UO_2L^{III}(H_2O)_n{\cdot}m(H_2O)]^+ + (5\text{-}n\text{-}m)H_2O \qquad (2)$$

Reaction (1) does not include the hydration effect, while reaction (2) takes into account the release/rearrangement of solvent molecules from the equatorial plane of the uranyl cation.

To help understand which coordination mode (mono-, bi-, or η^2) is the most probable in the $(UO_2L^{III})^+$ complex, it is more meaningful to compare the energies of the structure isomers (mono-, bi-, or η^2) that follow the same desolvation scheme, i.e., the same values of (5 - n - m) in reaction (2). The results in Table 3 show that for the hydrated structures optimized in PCM water, the most stable isomer is always the structure with the bidentate mode. For reaction (2) with the value of (5 - n - m) = 2, the ΔG (kcal mol^{-1}) follows the trend: bi- (-44.3) < η^2– (-39.9) < mono- (-38.4). For reaction (2) with the value of (5 - n - m) = 1, the ΔG (kcal mol^{-1}) follows the trend: bi- (-46.2) < mono- (-37.8) < η^2– (-36.0). For reaction (2) with the value of (5 - n - m) = 0, the ΔG (kcal mol^{-1}) follows the trend: bi- (-48.2) < mono- (-40.3) < η^2– (-38.1). In brief, DFT computation suggests that the bidentate structure (Figure 2a) is the most probable coordination mode in the $(UO_2L^{III})^+$ complex. Evidently, the formation of hydrogen bonding between a water molecule and the carbonyl oxygen atom in HL^{III} stabilizes the bidentate coordination mode.

Table 3. Free energies for the formation of the complexes (*a* to *l* in Figure 3) in the gas phase and PCM water. The reactions considered are $[UO_2]^{2+} + (L^{III})^- \rightarrow [UO_2L^{III}]^+$ for the formation of *a* - *c* and $[UO_2(H_2O)_5]^{2+} + (L^{III})^- \rightarrow [UO_2L^{III}(H_2O)_n{\cdot}m(H_2O)]^+ + (5\text{-n-m})H_2O$ for *d* – *l*.

Coord. Mode	Structure	n	5-n-m	ΔG, kcal mol^{-1}	
				Gas phase	PCM water
Monodentate	*a*	-	-	-351.3	-38.4
Bidentate	*b*	-	-	-392.2	-37.5
η^2	*c*	-	-	-360.0	-39.5
Monodentate	*d*	3	2	-205.1	-38.4
	e	4	1	-210.1	-37.8
	f	4	0	-223.2	-40.3
Bidentate	*g*	3	2	-226.4	-44.3
	h	3	1	-229.9	-46.2
	i	3	0	-238.7	-48.2
η^2	*j*	3	2	-214.6	-39.9
	k	3	1	-212.8	-36.0
	l	3	0	-223.5	-38.1

2.2 Vanadium complex with Glutaro-imide-dioxime

Structural studies on vanadium complexation with amidoxime ligand were conducted to help understand the extremely strong sorption of vanadium on poly(amidoxime) sorbents. An unusual “bare” V^{5+}/ complex with glutaroimide-dioxime was synthesized from aqueous solution. Multinuclear NMR, ESI-MS and EPR studies were performed to characterization the structure of the complex in solution. Data processing and summarization of the vanadium system are in progress and will be included in the next milestone report.

3. CONCLUSION

Glutarimidoxioxime (HL^{III}) and two other amidoxime-related ligands, glutarimidedioxime (H_2L^I) and glutardiamidoxime (H_2L^{II}), represent the three possible functionalities that could form in the radiation-induced grafting process to prepare the sorbents for the extraction of uranium from seawater. The results from this study, in conjunction with those from previous studies, suggest that the conditions of the grafting process (e.g., temperature, stoichiometric ratio of reactants) should be carefully selected and controlled to maximize the formation of glutarimidedioxime (H_2L^I), and probably glutardiamidoxime (H_2L^{II}) as well, but minimize the formation of glutarimidoxioxime (HL^{III}) because the binding strength of HL^{III} with U(VI) is eight orders of magnitude lower than that of H_2L^I and H_2L^{II}.

4. Publications in FY15

- **Chem. Eur. J., 2014, 20, 14499 – 14506.** F. Endrizzi, L. Rao, Formation of $Ca^{2+}$and Mg^{2+} Complexes with $(UO_2)(CO_3)_3^{4-}$ in Aqueous Solution: Effect on the Speciation of U(VI) and its Extraction from Marine Environments.
- **Polyhedron, 2015, 95, 54–59**. C. J. Leggett, L. Rao, Complexation of Calcium and Magnesium with Glutarimidedioxime: Implications for the Extraction of Uranium from Seawater.
- **Dalton Transactions, 2015, 44, 13763–14180.** F. Endrizzi, A. Melchoir, M. Tolazzi, L. Rao, Complexation of Uranium(VI) with Glutarimidoxioxime: Thermodynamic and Computational Studies.
- **Sep. Sci. Tech., in press**. X. Sun, P. Zanonato, P. Di Bernardo, Z. Zhang, L. Rao, Sorption of Uranium and Other Metal Ions on Amine-Functionalized Silica Materials.

5. ACKNOWLEDGMENTS

Funding for this work was provided by the Fuel Resources, Fuel Cycle Research and Development Program, Separations and Waste Form Campaign, Office of Nuclear Energy, of the U.S. Department of Energy under Contract Number DE-AC02-05CH11231 with Lawrence Berkeley National Laboratory.